



Huge multiple spinal extradural meningeal cysts in infancy

Kohei Tsuchimochi¹ · Takato Morioka² · Nobuya Murakami² · Fumiya Yamashita¹ · Nobuko Kawamura³

Received: 14 September 2018 / Accepted: 19 November 2018 / Published online: 23 November 2018
© Springer-Verlag GmbH Germany, part of Springer Nature 2018

Abstract

Background Multiple spinal extradural meningeal cysts (SEMCs) are rare lesions. SEMCs communicate with the subarachnoid space through multiple dural defects and expand into the extradural space with progressive spinal cord compression.

Case presentation We report a 5-month-old boy with hydronephrosis involving nine huge SEMCs that were distributed from the T1–L5 levels. Eight SEMCs, except for one small noncommunicating cyst, were exposed through laminoplastic laminotomy at the T10–L5 and T3–5 levels. Five transdural communications with dural defects were packed with a piece of autologous muscle and fibrin glue. Tenting sutures to lift up the dura to the vertebral arch were added to minimize the extradural dead space. Postoperatively, cord compression was relieved and hydronephrosis improved.

Conclusion In conclusion, packing of all dural defects and dural tenting sutures at a one-staged operation is useful in the surgical management of huge and multiple SEMCs in infancy.

Keywords Extradural arachnoid cyst · Spinal meningeal cyst · Multiple cystic lesion · Cyst removal

Introduction

A spinal extradural meningeal cyst (SEMC) is an uncommon lesion that communicates with the subarachnoid space through a small dural defect (or fistula) and expands into the extradural space with progressive spinal cord compression (Fig. 1a) [2, 6, 9]. The majority of dural defects are thought to be congenital in origin, although some can be acquired from trauma, infection, or inflammation [2, 3, 6, 9, 11]. The one-way valve mechanism of the cerebral spinal fluid (CSF) flow might

cause the arachnoid membrane to become herniated and enlarged in the extradural space [2, 3, 6, 9, 11]. Most SEMCs are located posteriorly in the spinal canal. This occurs because dural defects are commonly located in the posterolateral aspect of the dural sac, most frequently in the thoracic spine, at the armpit of the root sleeve. SEMC can be distributed far laterally, extending to the intervertebral foramen [1, 5, 11, 13, 14] (Fig. 1a).

Most SEMCs are solitary and multiple SEMCs are rare [2, 7, 12, 13, 15, 16]. Although the exact pathogenesis of multiple SEMCs is unknown, multiple SEMCs are characterized by multiple dural defects at the armpits of the dural sleeves, and multiple septa divide the cysts in a tandem arrangement [3, 13] (Fig. 1b). These SEMCs may extend in a rostro-caudal direction until they collide with adjacent cysts. Fibrovascular trabeculae in the epidural fat may intercept enlargement of these cysts, leading to septal formation, with or without communication through a hole in the septum [13]. Cases of multiple SEMCs have been reported in children and adolescents, typically with progressive paraparesis [2, 13, 15, 16]. We report a male infant with huge multiple SEMCs, in whom neurogenic bladder instead of motor disturbance was observed. The surgical strategy for multiple SEMCs in infancy is also discussed.

✉ Takato Morioka
takato@ns.med.kyushu-u.ac.jp

¹ Department of Pediatric Neurology, Fukuoka Children's Hospital, 5-1-1 Kashii-Teraha, Higashi-ku, Fukuoka 813-0017, Japan

² Department of Neurosurgery, Fukuoka Children's Hospital, 5-1-1 Kashii-Teraha, Higashi-ku, Fukuoka 813-0017, Japan

³ Department of Radiology, Fukuoka Children's Hospital, 5-1-1 Kashii-Teraha, Higashi-ku, Fukuoka 813-0017, Japan

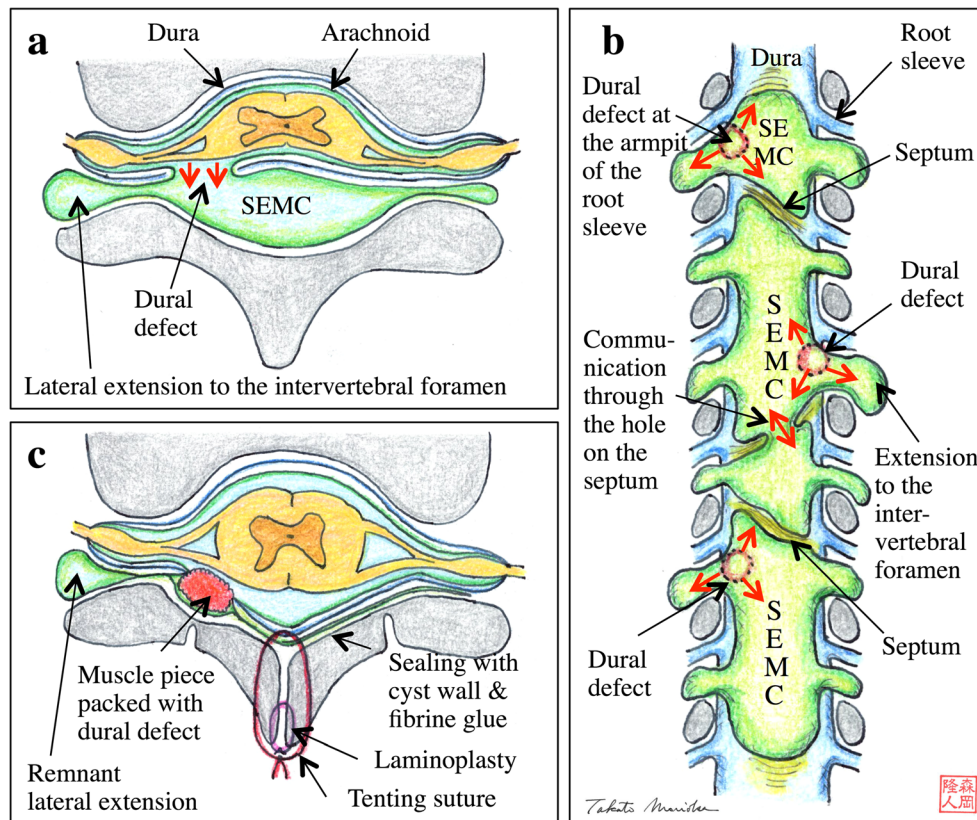
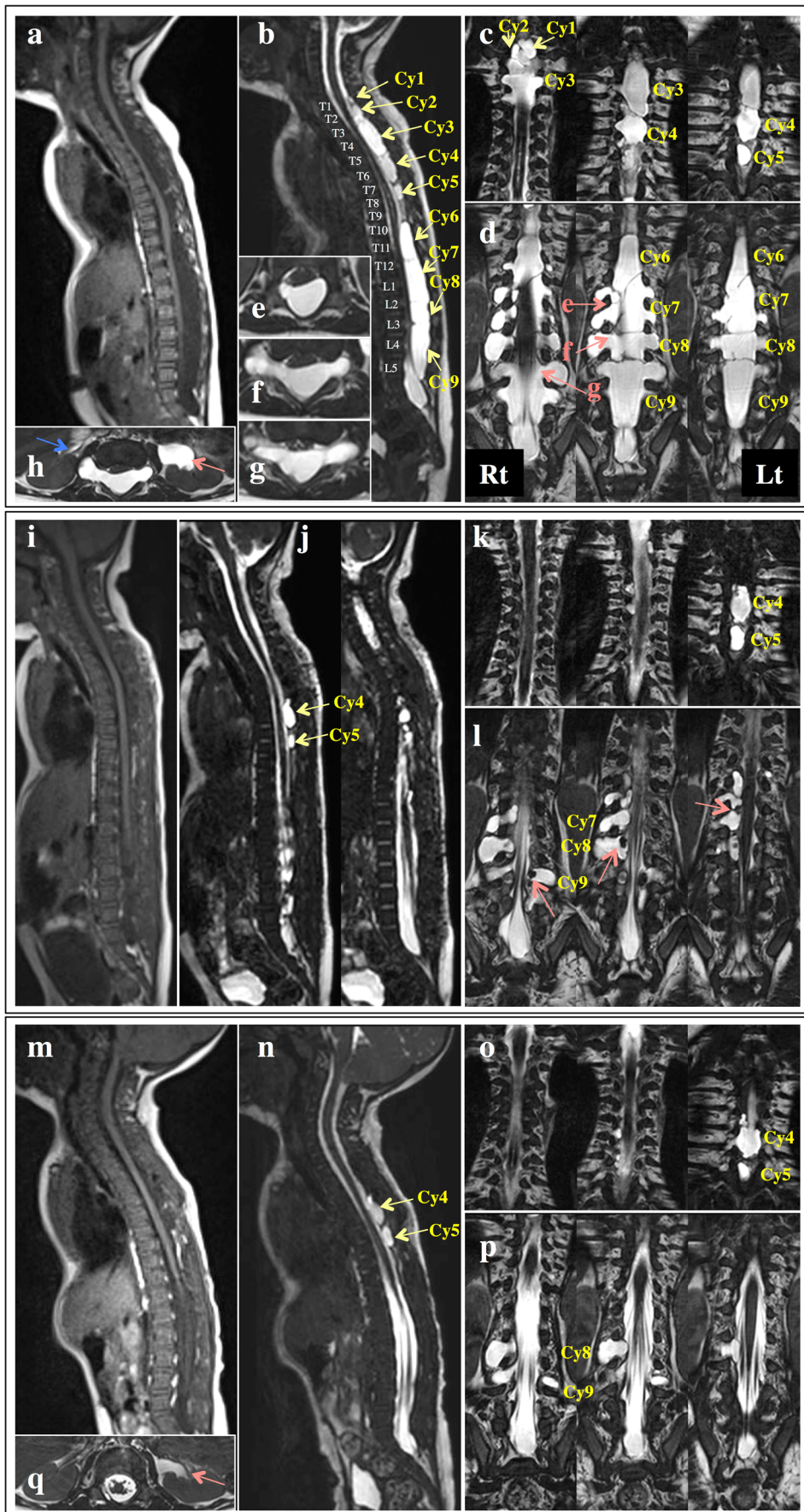


Fig. 1 **a** Schematic drawing of the pathophysiology of spinal extradural meningeal cysts (SEMCs). An SEMC communicates with the subarachnoid space through a dural defect (red arrows), which is commonly located in the posterolateral aspect of the dural sac, at the armpit of the root sleeve. The SEMC expands into the extradural space with progressive spinal cord compression, some of which extends far laterally into the intervertebral foramen. The dura and arachnoid membrane are indicated by blue and green, respectively. **b** Possible pathogenesis of huge multiple SEMCs. Multiple SEMCs originating from multiple dural defects (dotted red circles) at the armpit of the dural sleeve may extend in a rostro-caudal direction, until they collide with

adjacent cysts. Fibrovascular trabeculae in the epidural fat may intercept enlargement of the cysts, leading to septal formation, with or without intercystic communication through the hole. Multiple septa divide the cysts in a tandem arrangement. Red arrows indicate cerebrospinal fluid flow. **c** Schematic drawing of the surgical procedures for SEMCs. The dural defect is packed with an autologous piece of muscle. The dural surface is sealed with the remaining cyst wall and fibrin glue. This is lifted up at the mid-dorsal point to the lamina using tenting sutures to minimize the extradural dead space. Some lateral extension of the cyst may be remnant

Fig. 2 (a–h) Preoperative magnetic resonance imaging (MRI) at the age of 5 months. Sagittal views of (a) a three-dimensional T1-weighted spoiled gradient-recalled echo image (3D-T1) and (b) 3D heavily T2-weighted image using constructive interference in the steady state (CISS) show huge multiple cystic lesions posterior to the spinal cord at the T1–L5 levels. The cysts produce low- and high-signal intensity on 3D-T1 and CISS, respectively. On (b) sagittal and serial coronal CISS images of the (c) upper thoracic and (d) lower thoraco-lumbar regions, the cysts are divided into two groups: upper thoracic and lower thoracolumbar cysts. The upper thoracic cysts consist of five cysts (Cyst 1 [Cy1]–Cy5), forming a tandem arrangement from the T1–T6 levels. The lower thoracolumbar cysts consist of four cysts, which also form a tandem arrangement from T10–L5 levels, and strongly compress the cord. Some of the cysts show lateral extension into the intervertebral foramen. (e–g) Axial views of CISS, at the level of which dural defects were confirmed intraoperatively, fail to show dural defects of Cy7–9. Each slice level is indicated as red arrows in (d). (h) Axial view of a T2-weighted image (T2WI) shows severe hydronephrosis on the left (red arrow) and mild hydronephrosis on the right (blue arrow). (i–l) MRI on the 7th postoperative

day. Sagittal views of 3D-T1(i) and CISS (j) and a serial coronal view of CISS (k,l) show disappearance of multiple cysts in the vertebral column, except for Cy4–5, which do not compress the cord. Some of the lateral extension of Cy7–9 can still be seen. Red arrows indicate the muscle pieces packed with dural defects at the armpits of the root sleeves. (m–q) MRI at the 2nd postoperative month. Sagittal views of (m) 3D-T1 and (n) CISS, and a serial coronal view of (o, p) CISS show the disappearance of multiple cysts in the vertebral column, except for the small Cy4–5 without spinal cord compression. Serial coronal CISS images of the lower thoracolumbar regions show enlargement of the dural sac and good visualization of the cord and cauda equina. The degree of lateral extension of Cy7–9 is decreased. (q) Axial view of T2WI shows complete relief of right hydronephrosis. Left hydronephrosis has also improved (red arrow)



Case report

At birth, a boy had a dimple in the gluteal cleft. His neurological findings were grossly normal. However, at the age of 2 days, he developed a urinary tract infection. Hydronephrosis was observed on both sides, with more hydronephrosis on the left side. A conservative follow-up was performed because there did not appear to be any difficulty in urination and a vesicoureteral reflux was not noted on voiding cystography.

At the age of 5 months, magnetic resonance imaging (MRI), including three-dimensional heavily T2-weighted images using constructive interference in the steady state (CISS), showed nine cystic lesions (each cyst was labeled as Cyst 1 (Cy1)–Cy9, from the rostral to caudal sides) posterior to the cord at the T1–L5 levels (Fig. 2a, b). The cysts were divided into two groups at the T9 level as follows: upper thoracic and lower thoracolumbar cysts. The upper thoracic cysts consisted of five cysts (Cy1–5), which formed a tandem arrangement from the T1–T8 levels (Fig. 2b, c). Cy3 compressed the cord, while Cy5 was small and isolated from Cy4. The lower thoracolumbar cysts consisted of four cysts (Cy6–9), which also formed a tandem arrangement from T10–L5 levels and strongly compressed the cord. Most of these cysts showed far lateral extension into the intervertebral foramen (Fig. 2b, d). Combined use of sagittal, coronal, and axial CISS images (Fig. 2b–g) failed to show dural defects. Severe hydronephrosis on the left and mild hydronephrosis on the right were observed (Fig. 2h).

Surgery was performed at 6 months. First, Cy6–9 were exposed throughout laminoplastic laminotomy of T10–L5 (Fig. 3a). Four cysts were divided by three septa with fibrovascular tissue (Fig. 3b, c). Following longitudinal incision of the cyst wall, watery clear CSF spouted out. There was a communication between Cy6 and Cy7 through a hole in the septum (Fig. 3d, e). Three dural defects were observed at the armpits of the right T12, right L1, and left L2 root sleeves (Fig. 3f–h). Nerve roots were observed or herniated through each dural defect (Fig. 3f–h). Second, Cy3 was exposed through T3–5 laminotomy (Fig. 3i, j). Through a hole in the septa with Cy2 and Cy1, dural defects were observed at the armpits of left T2 and T1 root sleeves (Fig. 3k–m). Nerve roots were also observed or herniated through each dural defect (Fig. 3l, m). Because CSF was not aspirated from Cy4 (Fig. 3k), Cy4 was thought to be noncommunicating with the subarachnoid space. All of the five dural defects were packed with a piece of muscle and fibrin glue (Fig. 1c). The dural surface was also sealed with the remaining cyst wall and fibrin glue. The mid-dorsal dura was lifted up to the lamina using tenting sutures to minimize the extradural dead space (Fig. 1c).

Histologically, the cyst wall consisted of a fibrocollagenous, membranous tissue without neural tissue, which is compatible with the findings of meningeal cysts. Postoperatively, our patient

did not develop neurological deficits. MRI on the 7th postoperative day showed disappearance of multiple cysts in the vertebral column, except for Cy4–5, which did not compress the cord (Fig. 2i–k). Some of the lateral extension of Cy7–9 was still observed (Fig. 2l).

During the patient's 2-month postoperative follow-up, his development was normal. On MRI, visualization of the cord and cauda equina was good (Fig. 2m–p). Cy4–5 were still observed, but no spinal cord compression was observed (Fig. 2n). The degree of lateral extension of Cy7–9 was decreased (Fig. 2p). Right hydronephrosis was completely improved, and left hydronephrosis was also improved (Fig. 2q).

Discussion

Multiple SEMCs are rare and only four cases in pediatric patients have been published in the relevant literature [8, 13, 15, 16]. These multiple SEMCs occurred in a narrow age range from 8 to 14 years of age. The present infant was diagnosed as having hydronephrosis due to a neurogenic bladder at the age of 2 days and with multiple SEMCs at the age of 5 months. Therefore, our case is the youngest of the reported cases, and these SEMCs are thought to be congenital in origin.

Another unique aspect of the present case is the multiplicity and size of the SEMCs. There have only been four previous reports of more than five SEMCs in which each SEMC had a transdural communication through a dural defect or intercystic communication through a septal defect [7, 8, 13, 16]. In the present case, we detected nine cysts on preoperative CISS imaging. Eight cysts, except for a small Cy5, were recognized during surgery, and five dural defects and three septal defects were found. We previously reported [13] an 8-year-old boy who had 14 SEMCs at the T11–S1 levels. However, the cysts in the present case were distributed from the T1–L5 levels, which was a much larger area than that in any of the other previous reports.

As described in previous reports [1, 6, 11, 13, 14], in the present case, dural defects were observed at the armpits of the root sleeves during surgery. Preoperative CISS images, which have high spatial resolution and excellent contrast between CSF and solid structures, are useful for accurately localizing this communication [10, 13]. However, in the present case, CISS images failed to show the dural defects. The dural defects in our infant were too small to observe even on CISS images. Another possible reason is that herniated intradural roots packed the defect, as was observed intraoperatively. This also could have worked as a one-way valve mechanism.

The standard treatment for a solitary SEMC is cyst removal and watertight closure of transdural CSF communication through the dural defect [6, 9, 11]. However, surgery for multiple and huge SEMCs is more complex [7, 13, 16], especially in infancy. Our previous report [13] showed that simple removal of only the largest cyst left an extradural space between the

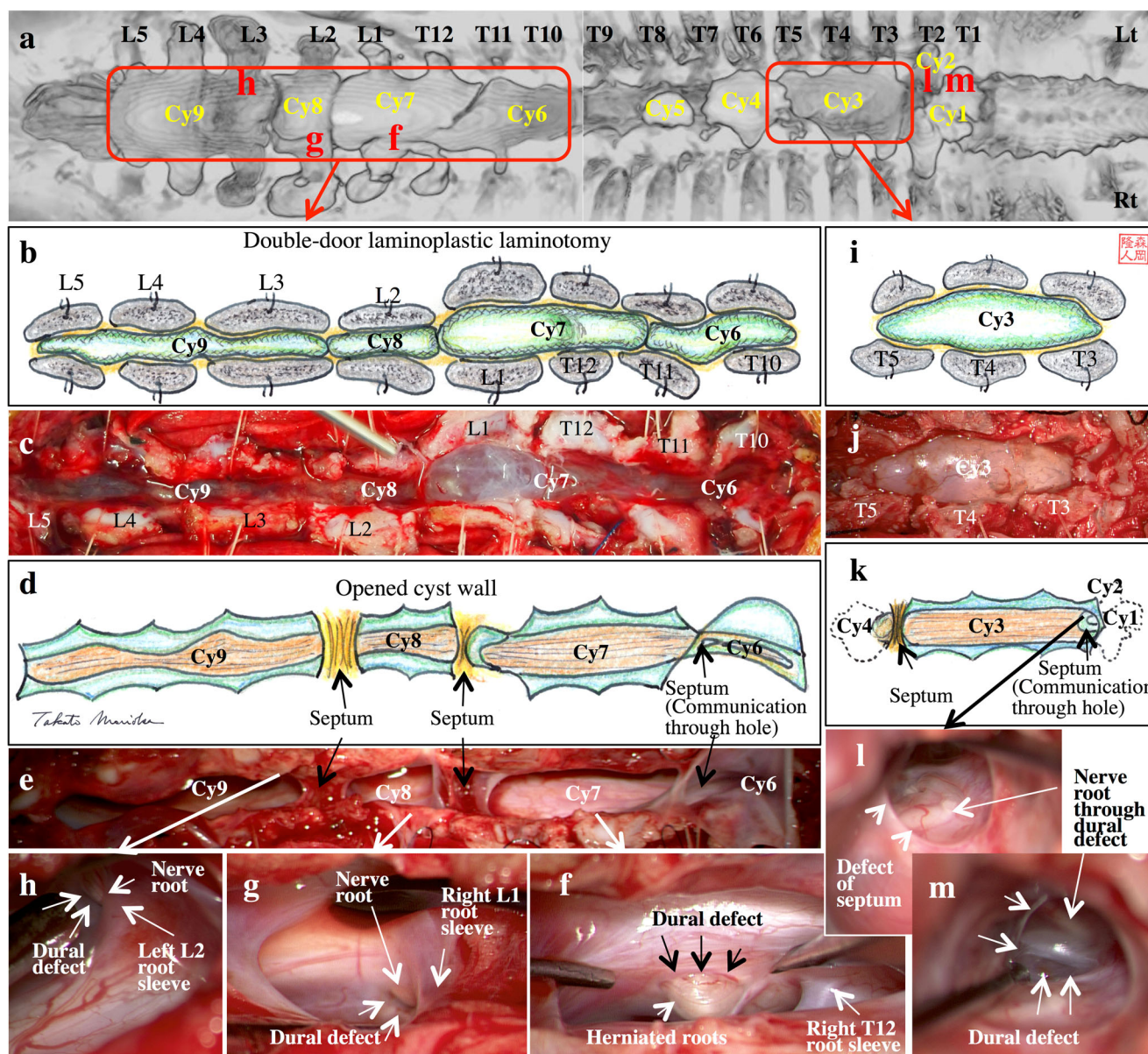


Fig. 3 Operative findings. (a) Three-dimensional reconstruction of coronal CISS images, which are shown in an orientation that matches with the subsequent operative view. Yellow text indicates the number of the cysts, and black text indicates the vertebral level. Two red boxes indicate the extent of the exposed operative field by laminotomies and red text indicates the position of the dural defects, which are shown in the following schematic drawings (b, d, i, k) and microscopic views (c, e–f, j, l, m) of the operative findings. (b, c) Cy6–9 at the lower thoraco-lumbar region were explored using double-door laminoplastic laminotomy of T10–L5. The cysts are filled with watery, clear cerebrospinal fluid. (d, e) Opening

of the cyst wall shows that Cy6–9 are divided by three septa with fibrocollagenous tissue. Communication between Cy6 and Cy7 was observed through a defect of the septum. Dural defects at the armpits of (f) right T12, (g) right L1, and (h) left L2 root sleeves can be seen. Nerve roots are (f) herniated or (g, h) seen through the dural defects. (i, j) Cy3 was exposed through T3–5 laminotomy. (k, l, m) Through a defect on the septa with Cy2 and Cy1, dural defects were observed at the armpits of the left T2 and T1 root sleeves. Nerve roots can be seen through the dural defects. Cy4 is punctured, but cerebrospinal fluid is not aspirated

remaining cysts. This extradural dead space was soon filled with leaked CSF, grew larger, and elicited spinal cord compression again. Therefore, removal of all SEMCs and closure of all dural defects at a one-staged surgery appear to be necessary [13]. However, extensive laminotomy from T1–L5 was too invasive for our infant in terms of intraoperative bleeding and subsequent kyphotic and scoliotic deformities [16]. All of the

lower thoracolumbar cysts (Cy6–9), which caused the neurogenic bladder, were fully exposed through T10–L5 laminotomy. However, for upper thoracic cysts, surgical manipulation of Cy1–4 was performed only through T3–T6 laminotomy. Because Cy5–6 were small and thought to be noncommunicating SEMCs [5], surgical manipulation was not performed.

Recent reports [3, 4, 15] have suggested that the closure of a dural defect without cyst resection is as effective as total resection of the cyst but less invasive. In our infant, the cyst wall was fragile and dissection of far laterally extended cysts was invasive in terms of bleeding from the decompressed paravertebral venous plexus [7]. When a dural defect is not amenable to suturing in a watertight fashion, a trial of patch grafting and fibrin glue repair is recommended [3, 6]. In the present infant, all of the five dural defects were packed with pieces of muscle and fixed with fibrin glue. The dural surface was also sealed with the remaining cyst wall. We consider that the use of tenting sutures to lift up the dura to the vertebral arch could help to avoid the re-accumulation of CSF in the extradural dead space in cases of huge, multiple SEMCs in infancy [13].

Using these methods, seven of nine SEMCs in the vertebral column were collapsed in our patient. Remnant noncommunicating Cy4 and Cy5 did not compress the cord. Lateral extension of Cy7–Cy9 was remnant, although decreased in size. The effect of mid-dorsal tenting sutures might not have reached the lateral sides (Fig. 1c). Further follow-up should be performed to confirm complete remission of multiple SEMCs in our patient.

Acknowledgments We thank Mr. Joji Hashimoto for providing excellent three-dimensional reconstructed images. We also thank Ellen Knapp, PhD, from Edanz Group (www.edanzediting.com/ac) for editing a draft of this manuscript. This work was partly supported by the Research Foundation of Fukuoka Children's Hospital.

Compliance with ethical standards

Conflict of interest The authors declare that they have no conflict of interest.

References

- Chen Z, Sun X-L, Zhao Y, Wang K, Jian F-Z (2014) Dural dissection cyst: a more accurate term for extradural meningeal cyst. *CNS Neurosci Ther* 20:515–520
- de Oliveira RS, Amato MCM, Santos MV, Simao GN, Machado HR (2007) Extradural arachnoid cysts in children. *Childs Nerv Syst* 23:1233–1238
- Fukumoto H, Samura K, Katsuta T, Miki K, Fukuda K, Inoue T (2016) Extensive multilobular spinal extradural meningeal cyst that developed 16 years after traumatic brachial plexus injury: a case report. *World Neurosurg* 86:510.e5–510.e10
- Funao H, Nakamura M, Hosogane N, Watanabe K, Tsuji T, Ishii K, Kamata M, Toyama Y, Chiba K, Matsumoto M (2012) Surgical treatment of spinal extradural arachnoid cysts in the thoracolumbar spine. *Neurosurgery* 71:278–284
- Liu JK, Cole CD, Sherr GT, Kestle JRW, Walker ML (2005) Noncommunicating spinal extradural arachnoid cyst causing spinal cord compression in a child. Case report. *J Neurosurg* 103(Pediatrics 3):266–269
- Liu JK, Cole CD, Kan P, Schmidt MH (2007) Spinal extradural arachnoid cysts: clinical, radiological, and surgical features. *Neurosurg Focus* 22:E6
- Marbacher S, Barth A, Arnold M, Seiler RW (2007) Multiple spinal extradural meningeal cysts presenting as acute paraplegia. Case report and review of the literature. *J Neurosurg Spine* 6:465–472
- Myles LM, Gupta N, Armstrong D, Rutka JT (1999) Multiple extradural arachnoid cyst as a cause of spinal cord compression in a child. Case report. *J Neurosurg* 91(1 Suppl):116–120
- Nabors MW, Pait TG, Byrd EB, Karim NO, Davis DO, Kobrine AI, Rizzoli HV (1988) Updated assessment and current classification of spinal meningeal cysts. *J Neurosurg* 68:366–377
- Nakagawa A, Kusaka Y, Jokura H, Shirane R, Tominaga T (2004) Usefulness of constructive interference in steady state (CISS) imaging for the diagnosis and treatment of a large extradural spinal arachnoid cyst. *Minim Invas Neurosurg* 47:369–372
- Oh JK, Lee DY, Kim TY, Yi S, Ha YY, Kim KN, Shi H, Kim DS, Yoon DH (2012) Thoracolumbar extradural arachnoid cysts: a study of 14 consecutive cases. *Acta Neurochir* 154:341–348
- Payer M, Bruhlhart K (2011) Spinal extradural arachnoid cyst: review of surgical techniques. *J Clin Neurosci* 18:559–560
- Samura K, Morioka T, Miyagi Y, Nagata S, Mizoguchi M, Mihara F, Sasaki T (2007) Surgical strategy for multiple huge spinal extradural meningeal cysts. Case report. *J Neurosurg* 107(4 Suppl Pediatrics):297–302
- Sun J-j, Wang Z-y, Teo M, Li Z-d, Wu H-b, Yen R-y, Zheng M, Chang Q, Liu IY (2013) Comparative outcomes of the two types of sacral extradural spinal meningeal cysts using different operation methods: a prospective clinical study. *PLoS One* 8:e83964
- Suryaningtyas W, Arifin M (2007) Multiple spinal extradural arachnoid cysts occurring in a child. Case report. *J Neurosurg* 106(2 suppl Pediatrics):158–161
- Takagaki T, Nomura T, Toh E, Watanabe M, Mochida J (2006) Multiple extradural arachnoid cysts at the spinal cord and cauda equine levels in the young. *Spinal Cord* 44:59–62